Study on Stabilization of Optical Fiber Interferometric Sensor

Shao Jie*, Chen Jian-yong**, Wu Zhi-zong, Tang Qian-jin
Laser and Optoelectronics Lab,
The Third Research Institute of the Ministry of Public Security, Shanghai, P.R. China

ABSTRACT

Optical fiber interferometric (OFI) sensors have been extensively used to measure a large variety of parameters due to their superior performance. The F-P OFI sensors are very sensitive to the cavity-length changes. However, it is difficult to fix the operating position at the quadrature point (Q point) in the sensor fabrication, and the sensor may also encounter with various environmental perturbations, which may drive the sensors out of the linear region. For the purpose of developing a highly-sensitive and reliable OFI vibration sensor, a new method was proposed and demonstrated in our research. By choosing a short cavity length, we can obtain OFI sensor with large interference period, which is helpful to avoid the infection of Q point drifting, but the visibility decline problem will arise simultaneously. A tilted diaphragm method was used to solve this problem in the short cavity length. Theoretical analyses have been performed, and a tilted diaphragm optical fiber sensor has been fabricated, the result shows a visibility of nearly 100% is realized in a short cavity about 50μm.

Keywords: OFI, Stabilization, Tilted diaphragm, Visibility

1. INTRODUCTION

Early fiber optical sensors for vibration signal detection were based mostly on fiber optic intrinsic interferometers such as all-fiber Michelson interferometers and Mach–Zehnder interferometers [1][2][3]. Either the reflections (Michelson) or the transmissions (Mach–Zehnder) of the light beams propagating in the two arms are recombined to generate interference signals that are modulated by the vibration. The intrinsic fiber interferometric sensors have shown high sensitivity when a long fiber was used in the sensing arm. However, they suffer from the fringe fading problems that result from random polarization rotation. They are also unstable because of drift in the source wavelength and temperature-induced path-length changes.

Fabry-Perot OFI (Optical fiber interferometric) sensors have been extensively used for the detection and measurement of a large variety of physical, chemical and biomedical parameters [4][5][6][7]. Compared with other types of fiber optic sensors, Fabry-Perot OFI sensors have the advantages of being simple and compact in size, insensitive to environmental fluctuations and none polarization-induced signal fading, being capable of point measurements with minimal cross sensitivity. F-P OFI sensors is fabricated with a small sensing element known as Fabry-Perot cavity formed by two parallel reflecting surfaces, which is formed by a single mode fiber tip and a MEMS silicon diaphragm.

The interference is typically a sinusoidal function of OPD. The highest sensitivity can be obtained at the quadrature point (Q point) [8][9]. A variety of diaphragm-based F-P OFI sensors have been developed and all of which operate in the linear region, the Q point of the probes must match the laser sources we used, sensors that operate in the linear region have the advantages of a linear transfer function, no ambiguity in fringe direction, simple signal processing. Confining the operation to the linear region places difficulty manufacturing constraints on the probe. Also the probe and sometimes the laser we uses will encounter with various environmental perturbations, which may drive the sensors out of the linear region. Two methods are put forward to solve this problem; one is change the wavelength of the laser sources to meet the environment changes, this method is proposed and demonstrated in our previous work [10]. More simply another method is to increases the stability and enlarges the linear region. The shorter the Fabry-Perot cavity, the larger interference fringe can be obtained, so the short F-P cavity length was used in this method. But meanwhile, short cavity length may

*jiesh@hotmail.com; Address: B zone, No. 339 Bisheng Road, Zhangjiang High-Tech Park, Shanghai, 201204, P.R. China.

**cjy@siom.ac.cn.

International Symposium on Photoelectronic Detection and Imaging 2009: Material and Device Technology for Sensors, edited by Xu-yuan Chen, Yue-lin Wang, Zhi-ping Zhou, Qing-kang Wang, Proc. of SPIE Vol. 7381, 73811V · © 2009 SPIE
CCC code: 0277-786X/09/$18 · doi: 10.1117/12.835590

fade the interference fringe and the visibility decline problem will arise simultaneously, the sensitivity become small accordingly. Fiber tip coating may solve this problem, but it may bring the coating randomicity when fabricating in such a small area [8]. In this paper we introduce a tilted diaphragm method to solve this problem. Based on the two beam interference theory, we deduce the interference intensity in the diaphragm condition, both the long interference period and the large fringe visibility could be gained by a proper tilt angler, by this means, the interference sensitivity and the dynamic range could be guaranteed. Based on the method we deduced, a tilted diaphragm probe was made and it shows a good appearance on the practical application.

2. METHOD OF OPERATION

The fiber optic sensor is illustrated schematically in Fig. 1. The system consists of a sensor probe, a laser source, a low-noise optical receiver, and single-mode fibers linking the sensor probe and the optical receiver. The light from a 1550 nm laser propagates along the fiber to the sensor head through a 2×2 3dB coupler. As shown in the enlarged view of the sensor probe (Fig. 1, inset), the lead in-out fiber and the thin silicon diaphragm are bonded together in a cylindrical fused silica tube to form an F-P sensing element. The incident light is first partially reflected at the end face of the lead in-out fiber. The remainder of the light propagates across the air gap to the inner surface of the diaphragm, where it is once again partially reflected. The diaphragm etalon formed by the two surfaces of the diaphragm had to be carefully treated in the OFI system.

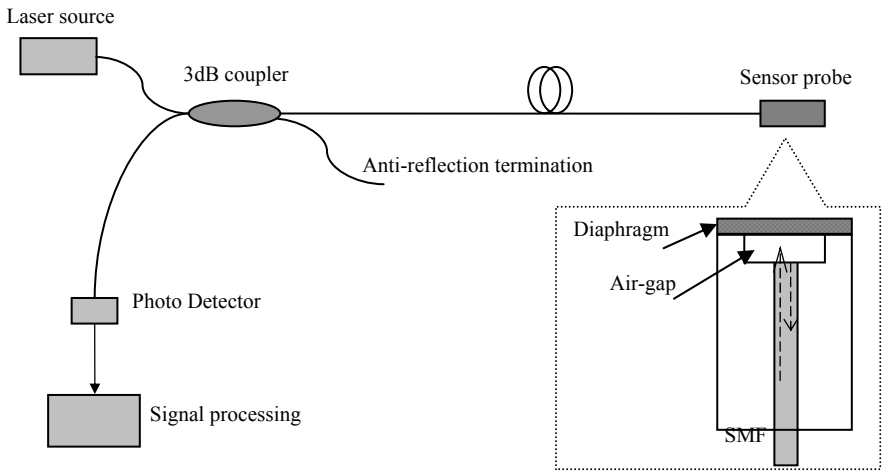

Fig. 1. Schematic of Fabry-Perot sensor system setup.

Fig. 2 is a theoretical calculation of the interference fringes to the cavity length changes. The F-P cavity used in this type of sensor usually can be considered as low finesse F-P interferometer. Only the first two beams need to be accounted in the process of interference which occurs inside the fiber tip, one is the beam reflected from the tip inside the fiber and the other is the beam emitted from the fiber, propagating through the cavity, returned and coupled into the fiber.

When cavity length has a little change, the interference fringe will shift horizontally. The laser should be locked in a stay wavelength when system is operating, and the intensity detecting from the PD will be changing like the bold line showed in Fig. 2. To ensure that system operates in a linear range, the laser wavelength should be in the region between two vertical lines. It can be easily figure out that a large interference period is helpful to make the sensor more stable, because system has a large linear operating range in this condition, and the sensor can operate without Q point tracking. The interference period and the cavity length are related by

$$PERIOD = \frac{\lambda^2}{2d} \tag{1}$$

where d is the cavity length. But the visibility decline problem will arise simultaneously by choosing a short cavity length simply without other consideration.

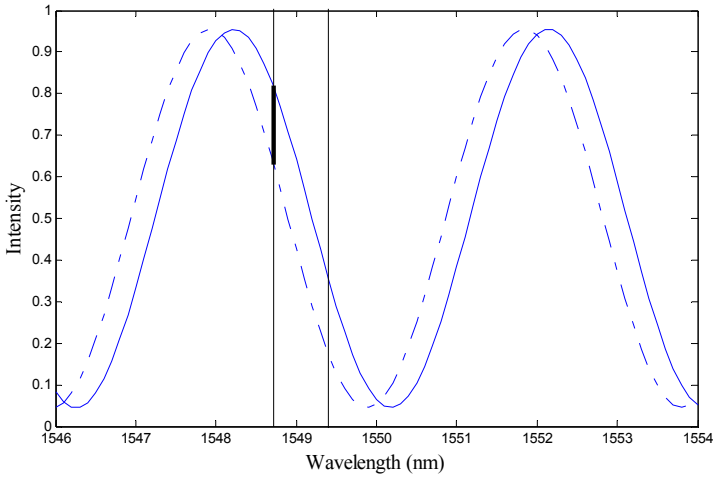

Fig. 2 Interference fringe changes as the small cavity length changes, d=280um, Δd=50nm, R_1=3.5%, R_2=95%

The total optical intensity two beams interfered can be expressed as

$$I = I_0\left[R_1 + 2\sqrt{TR_1R_2}(1-R_1)\cos(2kd+\pi) + TR_2(1-R_1)^2 \right] \tag{2}$$

Where I_0 is the optical input intensity, R_1 is the intensity reflectivity of the fiber tip and R_2 is the intensity reflectivity of the diaphragm. T is the power transmission coefficient that the beam coupled into the fiber, and can be obtained by the relation [11]

$$T = \left| \frac{1}{2P}\int_0^{2\pi} d\phi \int_0^{\infty} (E_x \times H_y)\vec{e}_z r dr \right|^2 \tag{3}$$

It is well known that the HE_{11} mode of a weakly guided step-index single-mode fiber are very nearly transverse and linearly polarized, it is accurately approximated by a Gaussian distribution [12],

$$E_{x'} = \sqrt{\frac{4\sqrt{\mu_0/\varepsilon_0}P}{\pi n_2 \omega_0^2}} \exp\left(-\frac{r^2}{\omega_0^2} \right) e^{-i\beta z} \tag{4}$$

and magnetic filed

$$H_y = E_{x'} \Big/ \sqrt{\mu/\varepsilon} \tag{5}$$

where P is the transmitted power of the HE_{11} mode beam, ω_0 is the waist of the Gaussian beam which can be approximated very closely by the empirical formula [11]

$$\frac{\omega_0}{a} = 0.65 + \frac{1.619}{V^{3/2}} + \frac{2.879}{V^6} \tag{6}$$

The beam ejecting from the fiber tip keeps Gaussian distribution, and propagates to the diaphragm, and then reflected to the fiber tip. The beam distribution can be expressed as

$$E_x = \sqrt{\frac{4\sqrt{\mu_0/\varepsilon_0}P}{\pi n_2 \omega^2}} \exp\left(-\frac{r^2}{\omega^2} \right) \exp\left\{ -i\left[kz - \tan^{-1}\frac{z}{z_0} + \frac{kr^2}{2R(z)} \right] \right\} \tag{7}$$

where

$$\omega = \omega_0\sqrt{1+\left(\frac{z}{z_0}\right)^2};\, z_0 = \frac{\pi\omega_0^2}{\lambda};\, R(z) = z\left(1+\frac{z_0^2}{z}\right) \tag{8}$$

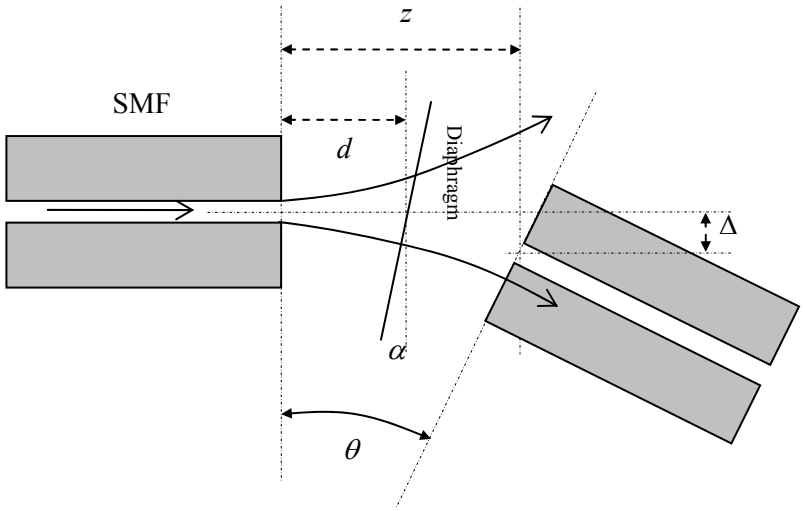

Fig. 3. Mirror imaging view shows the Gaussian beam interference Principle of tilted diaphragm F-P OFI

In this condition, the returned beam will be broadened according to formula (7) with z=2d, as shown in Fig. 3 by mirror imaging view.

According to the results in [11], the power transmission coefficient in the condition that fiber tilt and fiber offset can be expressed as follow independently

$$T_t = \left(\frac{2\omega_1\omega_2}{\omega_1^2+\omega_2^2}\right)^2 \exp\left[-\frac{2(\pi n_2\omega_1\omega_2\theta)^2}{\left(\omega_1^2+\omega_2^2\right)\lambda^2}\right] \tag{9}$$

$$T_o = \left(\frac{2\omega_1\omega_2}{\omega_1^2+\omega_2^2}\right)^2 \exp\left[-\frac{2\Delta^2}{\omega_1^2+\omega_2^2}\right] \tag{10}$$

Based on the formulas (9) and (10), we can easily obtain the power transmission coefficient when the fiber was tilted and offset simultaneously,

$$T = \left(\frac{2\omega_1\omega_2}{\omega_1^2+\omega_2^2}\right)^2 \exp\left[-\frac{2(\pi n_2\omega_1\omega_2\theta)^2}{\left(\omega_1^2+\omega_2^2\right)\lambda^2}\right]\exp\left[-\frac{2\Delta^2}{\omega_1^2+\omega_2^2}\right] \tag{11}$$

According to the Fig. 3, the misalignments after reflected by the diaphragm are θ=2α, Δ=$d$sin(2α)≈2$d\alpha$. Substituting the formula (8) into formula (11), and neglecting higher-order terms, we have

$$T = \frac{\left(1+\frac{4d^2}{z_0^2}\right)}{\left(1+\frac{2d^2}{z_0^2}\right)^2}.\exp\left[-\frac{4d^2\alpha^2}{\omega_0^2\left(1+\frac{2d^2}{z_0^2}\right)}\right].\exp\left[-\frac{4\pi^2\omega_0^2\left(1+\frac{4d^2}{z_0^2}\right)\alpha^2}{\left(1+\frac{2d^2}{z_0^2}\right)\lambda^2}\right] \tag{12}$$

When the diaphragm was not set to be tilted, which means α=0, the power transmission coefficient shows as

$$T = \left(1 + \frac{4d^2}{z_0^2}\right) \Big/ \left(1 + \frac{2d^2}{z_0^2}\right)^2 \tag{13}$$

According to formulas (2) and (12), the visibility of the interference fringe K can be expressed as

$$K = \frac{I_{\max} - I_{\min}}{I_{\max} + I_{\min}} = \frac{2\sqrt{TR_1R_2}(1-R_1)}{R_1 + TR_2(1-R_1)^2} \tag{14}$$

With the formulas (12), (13) and (14), the figure visibility vs. cavity length can be achieved. Fig. 4 are two theoretical curves of interference fringe visibility vs. cavity length, with R_1 = 3.5%, R_2 = 95%, λ=1550nm and ω_0 = 5.2 μm. When α=0, it is showing that the highest visibility is obtained near d= 280 μm. Setting the diaphragm tilted, which means change the α, with other parameters invariable, it can be seen that optimal visibility can be achieved in shorter cavity length when the α is increasing.

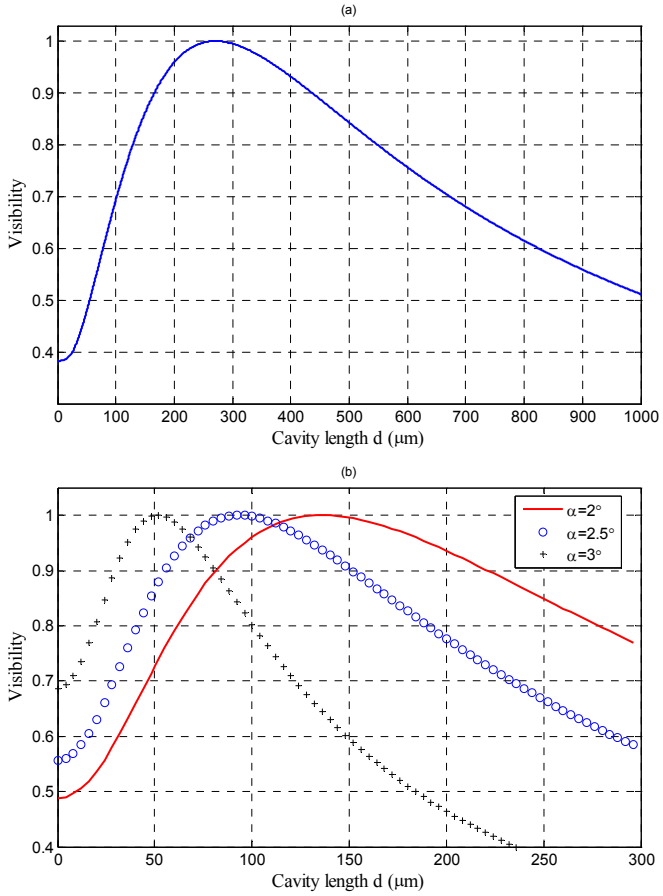

Fig. 4. Theoretical curves of fringe visibility for different Fabry-Perot cavity lengths. R_1 = 3.5%, R_2 = 95%, λ=1550nm and ω_0 = 5.2 μm. (a) Interference fringe visibility vs. cavity length when α=0; (b) Interference fringe visibility vs. cavity length when α=2°, 2.5°and 3°.

3. EXPERIMENTS

The experimental setup, as shown in Fig. 1, a 1550 nm semiconductor laser was used. The sensor head is composed of a silicon diaphragm and a lead in single mode fiber. The surface of silicon diaphragm was coated with designed

reflectivity. As analyzed above, a large interference period can be achieved by choosing a short cavity length. The experimental result was showed in Fig. 5.

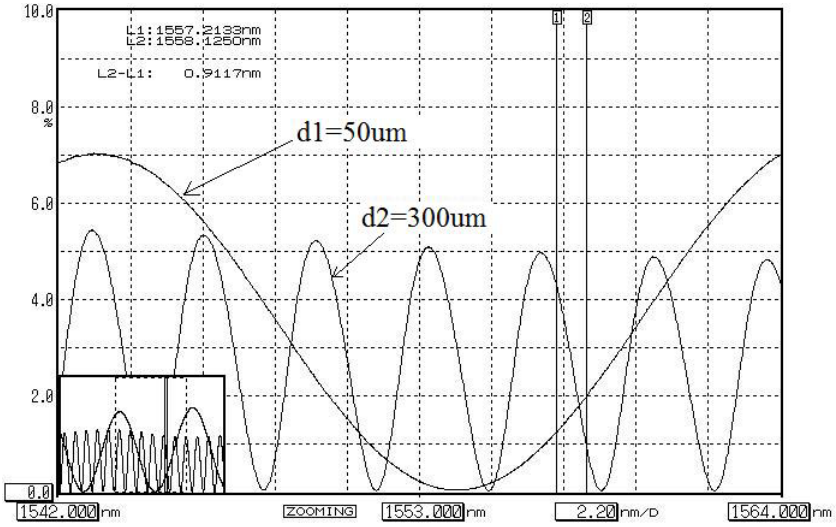

Fig. 5. Experimental results of interference fringe when cavity length was 50 μm and 300 μm.

Visibility of no tilted and tilted diaphragm was presented experimentally, as shown in Fig. 6. A distinct improvement of visibility was shown when using tilted diaphragm method. Using the short-cavity-length and tilted-diaphragm sensor probe, the system has a quite well stabilization without LD temperature controlling when the sensor head temperature was changed from 10℃ to 40℃.

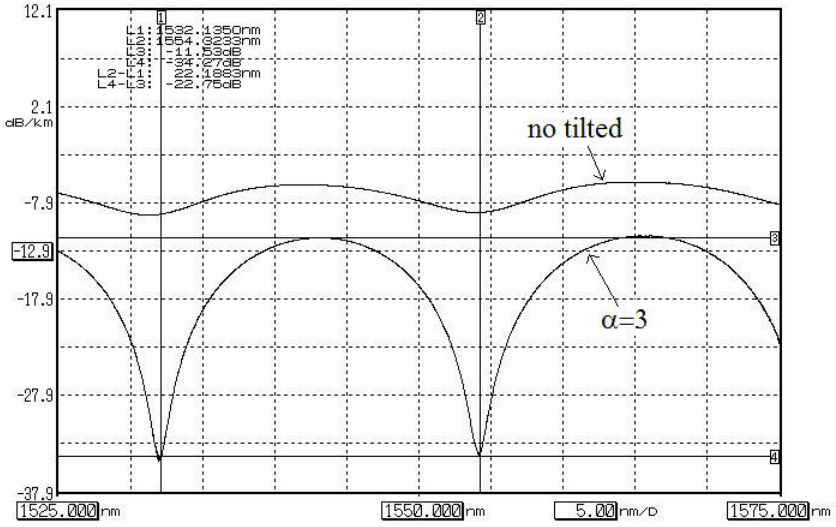

Fig. 6. Visibility of no tilted and tilted diaphragm.

4. CONCLUSION

In summary, the theory of an F-P OFI sensor has been proposed. The linearly dynamic range was broadened; improvements in the fringe visibility and sensitivity of the sensor have been made. A proper angler tilted diaphragm fiber optic probe was made without coating the fiber tip, which will not only simplify the sensor head fabrication, but also avoid the reflectivity of fiber tip variation. A visibility of nearly 100% was achieved in a large interference period, and the contrast experiment shows it can soundly guarantee both the dynamic range and the sensitivity of the probe. This

may effectively increase the environmental applicability and has a lower fabricated cost, can lead to a broad range of new applications.

REFERENCES

[1] D. A. Jackson, "Mono-mode optical fiber interferometers for precision measurement," J. Phys. E: Sci. Instrum. 18, 981-1001 (1985).

[2] Nadarajah N, Zhou Chonghua. Fiber optic acoustic sensor for non-destructive evaluation. Optics and Lasers in Engineering 22, 137-148 (1995).

[3] Fomitchov P A, Kromine A K. Sagnac type fiber optic array sensor for detection of bulk ultrasonic waves. IEEE Trannsactions on Ultrasonics, Ferroelectrics and Frequency Control 47(3), 584-589 (2000).

[4] R. A. Wolthuis, G. L. Mitchell, E. Saaski, J. C. Hartl, and M. A. Afromowitz, "Development of medical pressure and temperature sensors employing optical spectrum modulation," IEEE Trans. Biomed. Eng. 38, 974-981 (1991).

[5] Y. Kim and D. P. Neikirk, "Micro-machined Fabry–Perot cavity pressure transducer," IEEE Photon. Technol. Lett. 7, 1471-1473 (1995).

[6] A. Wang, H. Xiao, J. Wang, Z. Wang, W. Zhao, and R. G. May, "Self-calibrated interferometric-intensity-based optical fiber sensors," J. Lightwave Technol. 19, 1495-1501 (2001).

[7] Bing Yu, Dae Woong Kim, Jiangdong Deng, Hai Xiao, and Anbo Wang, "Fiber Fabry–Perot sensors for detection of partial discharges in power transformers" ,Appl. Opt. 42, 3241-3250 (2003).

[8] Bing Yu, Anbo Wang, "Grating-assisted demodulation of interferometric optical sensors", Appl. Opt. 42, 6824-6829 (2003).

[9] J.F. Dorighi, S. Krishnaswamy, J.D. Achenbach, Stabilization of an embedded fiber optic Fabry–Perot sensor for ultrasound detection, IEEE Trans. Ultrason. Ferroelectr. Freq. Control. 37, 820-824 (1995).

[10] Jianyong Chen, Dijun Chen, Jianxin Geng, Jun li, Haiwen Cai, Zujie Fang, "Stabilization of optical Fabry-Perot sensor by active feedback control of diode laser", Sensors and Actuators A. 148, 376-380 (2008).

[11] D. Marcus, "Loss analysis of single-mode fiber splices," Bell Syst. Tech. J. 56, 703–718 (1977).

[12] A. Yariv, Optical Electronics, 4th ed., Holt, Rinehart & Winston (1991).